CONF-920144--6

PNL-SA--19958

DE93 011690

THE EFFECTS OF AN AGGRESSIVE ENVIRONMENT ON THE SUBCRITICAL CRACK GROWTH OF A CONTINUOUS-FIBER CERAMIC COMPOSITE

C. H. Henager, Jr.
R. H. Jones

January 1993

Presented at the
16th Annual Conference on
Composites and Advanced
Ceramic Materials
January 8-10, 1992
Cocoa Beach, Florida

Prepared for
the U.S. Department of Energy
under Contract DE-AC06-76RLO 1830

Pacific Northwest Laboratory
Richland, Washington 99352

MASTER

DISCLAIMER

This report was prepared as an account of work sponsored by an agency of the United States Government. Neither the United States Government nor any agency thereof, nor any of their employees, makes any warranty, express or implied, or assumes any legal liability or responsibility for the accuracy, completeness, or usefulness of any information, apparatus, product, or process disclosed, or represents that its use would not infringe privately owned rights. Reference herein to any specific commercial product, process, or service by trade name, trademark, manufacturer, or otherwise does not necessarily constitute or imply its endorsement, recommendation, or favoring by the United States Government or any agency thereof. The views and opinions of authors expressed herein do not necessarily state or reflect those of the United States Government or any agency thereof.

DISTRIBUTION OF THIS DOCUMENT IS UNLIMITED

THE EFFECTS OF AN AGGRESSIVE ENVIRONMENT ON THE SUBCRITICAL CRACK GROWTH OF A CONTINUOUS-FIBER CERAMIC COMPOSITE

C. H. Henager, Jr. and R. H. Jones
Battelle, Pacific Northwest Laboratory, Battelle Blvd., Richland, WA 99352

Time-dependent crack growth measurements of ceramic composites in aggressive environments are being conducted on materials consisting of CVI SiC reinforced with Nicalon fibers (SiC/SiC$_f$) having C and BN fiber-matrix interfaces. Crack velocities are determined as a function of applied stress intensity. Results have been obtained for crack velocity-stress intensity relationships in pure Ar and in Ar plus 2000 ppm O_2 atmospheres at 1100°C. A 2D micromechanics model is used to represent the time-dependence of observed crack bridging events and is able to rationalize the observed phenomena.

INTRODUCTION

Ceramic matrix composites (CMCs) potentially offer high-strength, corrosion-resistant, high-temperature materials having a fracture resistance adequate for use as structural materials. Reinforcement of a brittle ceramic matrix material by brittle fibers or whiskers contributes to fracture resistance by reinforcement pullout, crack bridging, crack deflection, and matrix micro-cracking [1]. Fracture toughness values in the range of 20 to 30 MPa$\sqrt{m}$ can be achieved for continuous fiber-reinforced materials. However, the use of CMCs in systems requiring long-term environmental stability demands resistance to corrosion and time-dependent crack growth [2-7]. Time-dependent crack growth (subcritical crack growth) likely controls the long-term life of these materials when pre-existing flaws are present. Thus, methods of life prediction require an understanding of the processes controlling the time-dependent failure of CMCs.

Environmental effects on subcritical crack growth at elevated temperatures are specific concerns for CMC materials. CMCs rely on the intrinsic properties of the matrix, as well as the reinforcing materials, for corrosion resistance and high-temperature utility. Crack wake bridging by long fibers in continuous fiber reinforced CMCs dominates the mechanical response of these materials [1]. Therefore, the time-dependent response of the bridging zone at elevated temperatures would appear to be the dominant mechanism affecting subcritical crack growth in CMCs. Crack bridging reinforcements will be exposed to the environment and will be highly stressed. The environment can affect the bridging

reinforcements by penetration down the reinforcement-matrix interface. Fracture resistance due to crack bridging may be degraded due to environmental damage of the reinforcement-matrix interface. Degradation of the bridging reinforcements and the exposed fiber/matrix interface may increase subcritical crack growth velocities and decrease component lifetimes.

There is no data on the subcritical crack growth rates of CMC materials as a function of temperature or environment. Thus, this study has focussed on acquiring crack velocity data as a function of stress intensity, temperature, and environment. Data are presented for subcritical crack growth measured in a chemical-vapor infiltrated (CVI) β-SiC matrix material containing 8 laminates of Nicalon fiber cloth using tests at 1100°C in gaseous environments.

EXPERIMENTAL PROCEDURES

Composites consisting of Nicalon fiber cloth (0°/90°) and CVI β-SiC with both carbon (C) and boron nitride (BN) interfaces were tested. The composites are 8-ply material, 4 mm thick, fabricated by RCI of Whittier, CA. Interfaces of 1.0 μm C and 0.4 μm BN (nominal thicknesses) were deposited on the Nicalon fibers before the β-SiC CVI fabrication step. Single-edge-notched bend bar (SENB) specimens with dimensions of 4 mm x 5.5 mm x 50 mm were prepared. The SENB specimens were tested in 4-point bending using a fully articulated SiC bend fixture. The tests were performed inside a sealed mullite ceramic tube using a split clamshell furnace. A gas mixing manifold and gas flow controllers were used to establish and control the gas atmospheres during the test. Pure Ar and pure O_2 gas were mixed in the desired quantities using an MKS Type 147B four channel mass flow/pressure programmer with an MKS Type 250B pressure controller. The gas mixing ratios were set using a Thermox oxygen analyzer, and the manifold pressure was feedback-controlled to achieve a gas flow rate of ~1.6×10^{-6} m^3/s.

The subcritical crack growth (SCG) studies were performed using stepped load tests with load holding carried out at 1100°C in argon and argon plus 2000 ppm O_2. To establish the matrix cracking loads and peak loads, SENB specimens were tested to failure at 1100°C in Ar at a strain rate of 1.6×10^{-5} s^{-1}. The SCG SENB specimens were then loaded below the matrix cracking stress, typically at an applied stress intensity of 7-8 MPa$\sqrt{m}$, to begin the test. The specimens were held at each load for 1000 s and the load was then increased to correspond to a stress intensity increase of about 1 MPa$\sqrt{m}$. This loading continued until a load drop was observed and the test was stopped. SCG specimens that were tested in Ar plus 2000 ppm O_2 were brought up to temperature in pure Ar.

RESULTS

SENB specimens of each of the C and BN interface CMCs were tested in 4-point bending at 1100°C in Ar to calculate a peak load fracture toughness value, K_Q, and to calculate a crack growth resistance curve, the R-curve. K_Q is calculated from

$$K_Q = \sigma_{max}\ a^{0.5}\ Y(\alpha) \qquad (1)$$

where σ_{max} is the outer-fiber bending stress at peak load, a is the crack length, α is the thickness normalized crack length, and $Y(\alpha)$ is the geometry factor for the SENB specimen in pure bending [8]. K_Q values of 17.3 and 15.1 MPa$\sqrt{m}$ were obtained for the C- and BN-interface materials at 1100°C in Ar, respectively.

It is more appropriate to calculate fracture toughness as a function of crack length in composite materials to determine the R-curve. This curve was calculated by using the measured specimen compliance to give a crack length and then using eq. 1 to calculate K. The SENB compliance depends on α as [9]

$$C(\alpha) = C(0) + \frac{2}{B\,E'}\int_0^{\alpha} (Y'(\alpha))^2\, d\alpha \qquad (2)$$

where C(0) is the compliance of an unnotched bar in 4-point bending given by [10], and B is the specimen width, E' is $E/(1 - \nu^2)$, and $Y'(\alpha)$ is given by

$$Y'(\alpha) = \frac{3S_1}{4W}\,\alpha^{1/2}\,Y(\alpha) \qquad (3)$$

S_1 is the lower support span of the bend fixture and W is the specimen thickness. The measured compliance of the notched specimen during the linear portion of the load-deflection curve is used to calculate the value of E'. The calculated R-curve indicated that K increased from 10 MPa$\sqrt{m}$ to ~27 MPa$\sqrt{m}$ as α increased from 0.3 to 0.5.

Each SCG test consists of a series of 1000 s-constant-load tests in 4-point bending at a constant temperature. The load-displacement curve for a typical test is shown in Figure 1 and the displacement-time curve for one of the 1000 s-exposures at constant load is shown in Figure 2. The logarithmic-shaped curve in Figure 2 indicates that the specimen displacement, and thus the crack opening displacement, undergoes a transient period of rapid displacement and attains a steady-state rate of displacement. The slope of the steady-state region beyond the transient is proportional to the crack velocity.

Writing $\delta = P\,C(\alpha)$, where δ is the displacement and P is the load, can be used to give

$$\frac{\partial \delta}{\partial t} = \frac{\partial}{\partial t}(P\,C(\alpha)) = P\,\frac{\partial C \partial \alpha}{\partial \alpha\ \partial t} = \frac{P}{W}\,\frac{\partial C}{\partial \alpha}\,\frac{da}{dt} \qquad (4)$$

which is then used to derive the following expression for da/dt (V_c)

$$\frac{da}{dt} = V_c = \frac{\dot{\delta} W}{P\, C'(\alpha)} \qquad (5)$$

where V_c is the crack velocity. $C'(\alpha)$ is calculated using eq. (2) and $d\delta/dt$ is the slope of the displacement-time curve in the steady-state region. The crack length is calculated from the measured specimen compliance by inverting eq. (2).

The data for the C- and BN-interface materials, when plotted as crack velocity versus applied stress intensity (V-K curves), reveal a stage II region where the crack velocity is essentially independent of the applied stress intensity (Figures 3 and 4) followed by a stage III, or power-law breakdown region, at high stress intensities. Presumably, a stage I threshold region exists at lower stress intensities, but is not observed in this data.

The breakdown region, stage III, exhibits a strong dependence on applied stress intensity and is always followed by a load drop and large crack extension on the next load increase. In some cases, the specimen fails before accelerated cracking is observed (Figure 4). The stage II region exhibits a very weak dependence on the applied stress intensity. The data reveal a slight increase in stage II crack velocity due to the presence of 2000 ppm oxygen in the gas. Also, the stress intensity required for the onset of stage III is shifted to lower value of the applied stress intensity. The shift is more pronounced for the BN-interface material compared to the C-interface material.

DISCUSSION AND MODELLING OF RESULTS

Subcritical crack growth data for monolithic ceramics does not show any stage II behavior, rather the crack velocity is observed to be a strong function of applied stress intensity [4-7]. This is usually expressed as a power-law such as $V = AK^n$, with the exponent on K in the range of 10 to 30. The observed stage II region exhibits a very weak dependence on applied stress intensity with exponents less than one. This behavior suggests that subcritical cracking in CMC materials is controlled by crack-bridging by the continuous fibers in the crack wake. The bridging zone acts to screen, or shield, the crack-tip from the applied stress intensity. Over the region of increasing K as a function of increasing crack length, a bridging zone is established for these materials and acts to screen the crack-tip from the applied stress intensity, K_{app}. A nearly constant crack-tip stress intensity, K_{tip}, is established as the bridging zone develops and R-curve behavior is observed. Eventually, the bridging zone saturates and cannot continue to shield the crack-tip from K_{app}. K_{tip} increases on increasing K_{app} once this limit is reached and cracking is accelerated resulting in the stage III breakdown region.

The evidence for bridging zone domination of subcritical crack growth comes partly from experiments using argon plus oxygen in comparison with pure argon and partly from a micromechanical model developed for this work. The addition of 2000 ppm oxygen to the 1100°C argon environment increases the crack velocity in the stage II regime and shifts the stage II-stage III transition to lower K values (Figures 3 and 4). The shift to lower K values for the transition to stage III

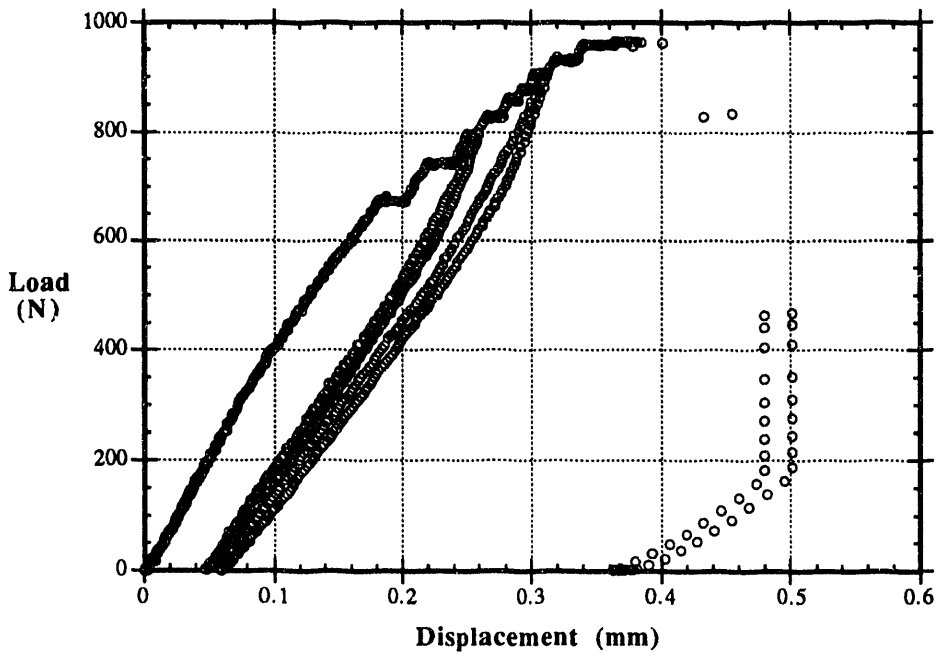

Figure 1. Load-displacement curve for typical subcritical crack growth test at 1100°C.

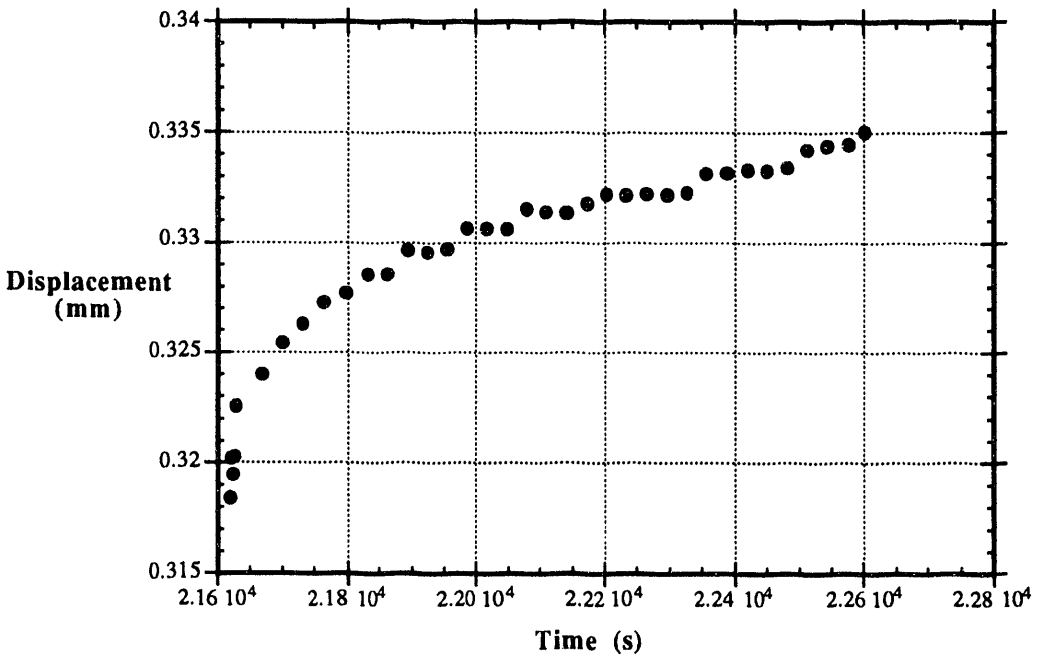

Figure 2. A displacement-time curve observed for a single load step for a BN-interface material during a subcritical crack growth test at 1100°C.

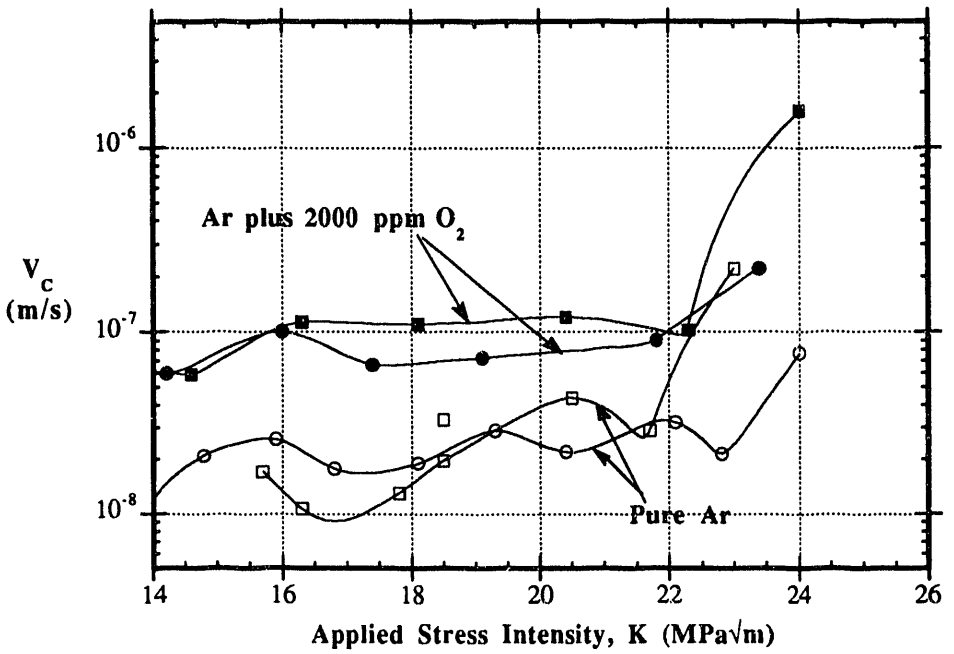

Figure 3. Crack velocity as a function of applied stress intensity (V-K) data for C-interface material at 1100°C in pure Ar and Ar plus 2000 ppm oxygen.

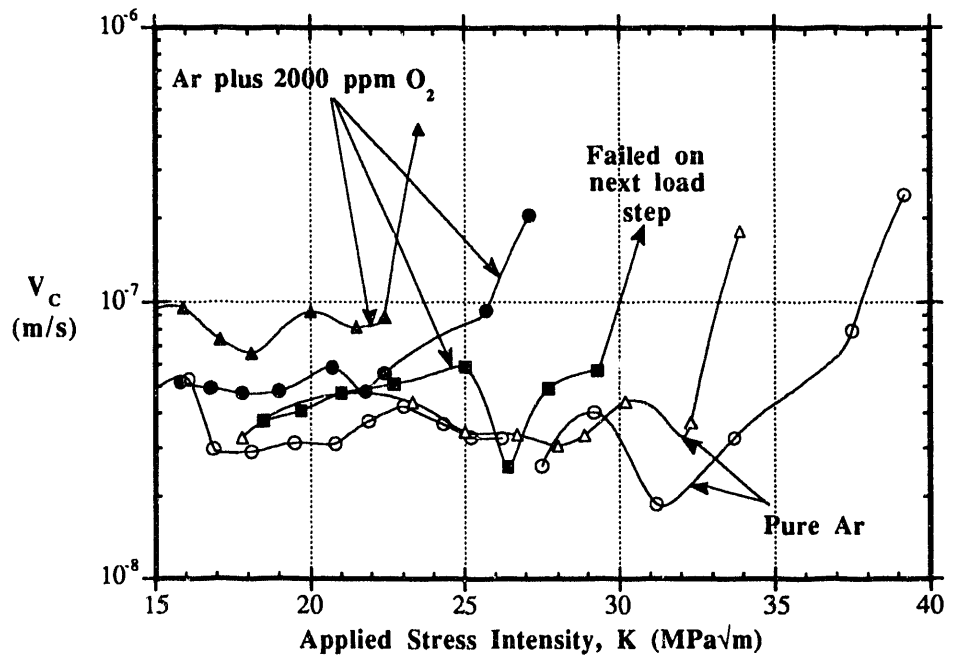

Figure 4. Crack velocity as a function of applied stress intensity (V-K) data for BN-interface material at 1100°C in pure Ar and Ar plus 2000 ppm oxygen.

crack growth is consistent with a reduction in the closure forces imparted on the crack faces by the bridging fibers. SEM photomicrographs (not shown here) of the CMCs exposed to the 2000 ppm O_2 plus argon reveal the partial removal of the C and BN-interfaces due to oxidation of these interface materials at 1100°C. The removal of this interface material would reduce the shear strength of the interface, reduce the ability of the matrix to transfer load to the fibers, and reduce the bridging zone effectiveness.

These same effects are demonstrated using a 2D-micromechanical model of a crack in a CMC material. The model places a semi-infinite crack in a linear-elastic body and simulates the bridging fibers by crack closure forces placed along the crack face. The forces applied by the fibers to the crack face are calculated using an explicit frictional bridging model [11] that calculates the fiber load transfer as a function of distance from the crack-tip. A basic result of the model is the prediction of crack-tip screening over a range of crack extension (R-curve) when high-strength fibers and weak interfaces are present.

The 2D-micromechanical model can also be used to explore the time-dependence of crack growth by allowing the crack-closure forces to undergo time-dependent relaxation. A bridged crack of a fixed bridging zone length is simulated using the model and the crack-closure forces are allowed to vary as shown in Figure 5. The crack velocities are calculated using an assumed V-K power law relationship with a stress intensity exponent of 10. A reduction in the crack-closure (fiber bridging) forces as a function of time, due to either stress relaxation in the fibers or creep/sliding of the interface, allows the crack to extend during the load step. The shape of the displacement-time curve (Figure 2) indicates that a logarithmic relaxation process is occurring. This relaxation process would be faster for the oxygen containing environment because the fiber/matrix interface is being selectively removed by oxidation. This process would reduce the fiber/matrix interfacial shear strength as a function of time. A faster relaxation shifts the onset of accelerated cracking (stage III) to lower K_{app} values and increases the relative crack velocities in the stage II region (Figure 5). This behavior agrees well with the experimental findings.

SUMMARY AND CONCLUSIONS

Subcritical crack growth in continuous-fiber CMC materials at 1100°C in pure Ar exhibits a stage II region where crack velocity depends weakly on the applied stress intensity. At higher stress intensities the crack velocity is accelerated and a stage III region is observed where crack velocity depends strongly on stress intensity. The stage II region corresponds to the development of the fiber bridging zone in the wake of the crack. It was shown that crack velocities are increased at 1100°C in Ar plus 2000 ppm oxygen compared to pure Ar. It was also observed that the oxygen-containing gas shifted the onset of stage III to lower values of applied stress intensity. These observations were rationalized using a 2D-micromechanical model developed to simulate cracks bridged by continuous fibers. SiC/SiC(f) composites are sensitive to environmental effects because their mechanical response is dominated by a crack wake bridging zone which is completely exposed to the environment. More severe environments that corroded the reinforcing fibers or the interfaces would be potentially very deleterious.

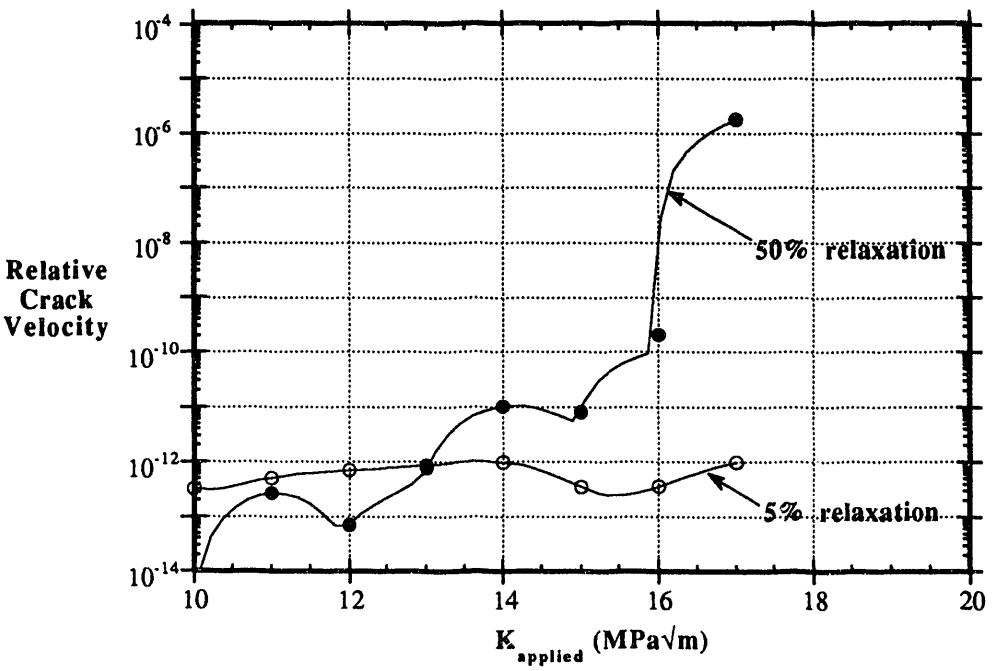

Figure 5. V-K predictions of the micromechanical model simulating a bridged crack and allowing the crack-closure forces to relax the indicated amounts in 1000 s.

ACKNOWLEDGMENTS

This work was supported by Basic Energy Sciences under U. S. Department of Energy (DOE) Contract DE-AC06-76RLO 1830 with Pacific Northwest Laboratory, which is operated for DOE by Battelle Memorial Institute.

REFERENCES

1. A. G. Evans, "Perspective on the Development of High-Toughness Ceramics", J. Am. Ceram. Soc., 73, 187-206 (1990).
2. J. L. Smialek and N. S. Jacobson, "Mechanism of Strength Degradation for Hot Corrosion of α-SiC," J. Am. Ceram. Soc., 69, 741-752 (1986).
3. D. C. Larsen, J. W. Adams, S. A. Bortz, and R. Ruh, "Evidence of Strength Degradation by Subcritical Crack Growth in Si_3N_4 and SiC," Fracture Mechanics of Ceramics V.6, R. C. Bradt et al., eds., Plenum Press, NY, 1983, pp. 571-585.

4. J. L. Henshall, "The Mechanism and Mechanics of Subcritical Crack Propagation in Hot-Pressed SiC Above 1000C," Advances in Fracture Research (Fracture 81), D. Francois, ed., Pergamon Press, NY, 1981, pp. 1541-1549.
5. H. Cao, B. J. Dalgleish, C. Hsueh, and A. G. Evans, "High Temperature Stress Corrosion Cracking in Ceramics," J. Am. Ceram. Soc., 70, 257-264 (1987).
6. C. H. Henager, Jr. and R. H. Jones, "Environmental Effects on Slow Crack Growth in Silicon Nitride", Ceramic Eng. Sci. Proc., V. 9 [9-10], 1525-1530 (1988).
7. C. H. Henager, Jr. and R. H. Jones, "Molten Salt Corrosion of Hot-Pressed Si_3N_4/SiC-Reinforced Composites and Effects of Molten Salt Exposure on Slow Crack Growth of Hot-Pressed Si_3N_4," in Corrosion and Corrosive Degradation of Ceramics, Ceramic Transactions, V. 10, R. E. Tressler and M. McNallen, eds., American Ceramics Society, Westerville, OH, 1990, pp. 197-210.
8. J. P. Bentham and W. T. Koiter, "Asymptotic Approximations to Crack Problems", in Methods of Analysis and Solutions of Crack Problems, G. C. Sih, ed., Noordhoff, Leyden, The Netherlands, 1973, pp. 131-178.
9. P. A. Whithey and P. Bowen, "Analysis of Chevron Notches in Pure Bending", Int. J. Fracture, 46, R55-R59 (1990).
10. J. I. Bluhm, "Slice Synthesis of a Three Dimensional 'Work of Fracture' Specimen", Engr. Fracture Mech., 7, 593-604 (1975).
11. A. G. Evans and R. M. McMeeking, "On the Toughening of Ceramics by Strong Reinforcements," Acta Metall., V. 34, 2435-2441 (1986).

DATE
FILMED
6/17/93